

NONTHERMAL RADIATION FROM CLUSTERS OF GALAXIES: THE ROLE OF MERGER SHOCKS IN PARTICLE ACCELERATION

STEFANO GABICI

Dipartimento di Astronomia e Scienza dello Spazio, Università di Firenze, Largo E. Fermi 5, I-50125 Florence, Italy;
 gabici@arcetri.astro.it

AND

PASQUALE BLASI

INAF/Osservatorio Astrofisico di Arcetri, Largo E. Fermi 5, I-50125 Florence, Italy; blasi@arcetri.astro.it

Received 2002 July 22; accepted 2002 October 7

ABSTRACT

Nonthermal radiation is observed from clusters of galaxies in the radio, hard X-rays, and possibly in the soft X-ray/UV bands. While it is known that radiative processes related to nonthermal electrons are responsible for this radiation, the sites and nature of particle acceleration are not known. We investigate here the acceleration of protons and electrons in the shocks that originated during mergers of clusters of galaxies, where the Fermi acceleration may work. We propose a semianalytical model to evaluate the Mach number of the shocks generated during cluster mergers, and we use this procedure to determine the spectrum of the accelerated particles for each one of the shocks produced during the merger history of a cluster. We follow the proton component, accumulated over cosmological timescales, and the short-lived electron component. We conclude that efficient particle acceleration, resulting in nonthermal spectra that compare with observations, occurs mainly in minor mergers, namely, mergers between clusters with very different masses. Major mergers, often invoked to be sites for the production of extended radio halos, are found to have on average too weak of shocks and are unlikely to result in appreciable nonthermal activity.

Subject headings: acceleration of particles — galaxies: clusters: general —
 radiation mechanisms: nonthermal — shock waves

1. INTRODUCTION

Rich clusters of galaxies are strong X-ray sources with luminosity typically in the range $L_X \sim 10^{43}$ – 10^{45} ergs s^{−1}. The X-ray emission is well explained as bremsstrahlung radiation of the very hot ($T \sim 10^8$ K), low-density ($n_e \sim 10^{-3}$ cm^{−3}), highly ionized intracluster electron gas.

There is now compelling evidence for the existence, besides the thermal electron gas, of a nonthermal population of particles, responsible for extended synchrotron radio halos in a growing fraction of the observed clusters (see Feretti et al. 2000 for a recent review) as well as for hard X-ray (HXR) and extreme-ultraviolet (EUV) excesses detected in a few clusters (see, e.g., Fusco Femiano et al. 1999, 2000; Lieu et al. 1996). While it is clear that radio emission is due to synchrotron radiation from relativistic electrons, it is not as clear how these particles are accelerated. Several models have been proposed, based on shock acceleration of electrons in merger shocks (Roettiger, Burns, & Stone 1999; Sarazin 1999; Takizawa & Naito 2000; Fujita & Sarazin 2001), models in which electrons are secondary products of hadronic interactions (Dennison 1980; Colafrancesco & Blasi 1998; Blasi & Colafrancesco 1999; Dolag & Ensslin 2000), and finally models in which electrons are continuously reenergized by turbulence (Schlickeiser, Sievers, & Thiemann 1987; Brunetti et al. 2001; Ohno, Takizawa, & Shibata 2002).

HXR and EUV radiation in excess of the thermal emission may be generated by inverse Compton scattering (ICS) of relativistic electrons off the photons of the cosmic microwave background radiation. When applied to the Coma Cluster, these models require values of the volume-averaged

magnetic field that are smaller than those measured through Faraday rotation, which are typically of several microgauss (Eilek 1999; Clarke, Kronberg, & Böhringer 1999). This conclusion can be possibly avoided only by constructing models in which a cutoff in the electron spectrum is tuned up in order to reduce the corresponding synchrotron emission. In these cases the magnetic field can be as high as 0.3–0.4 μ G (Brunetti et al. 2001). In the case of a secondary origin for the radiating electrons, the small magnetic fields imply a large cosmic-ray content in the intracluster gas. In the case of the Coma Cluster, the gamma-ray upper limit found by Sreekumar et al. (1996) is exceeded by the gamma-ray flux from the decay of neutral pions, as shown by Blasi & Colafrancesco (1999).

The HXR excess might also be the result of bremsstrahlung emission from a population of thermal electrons whose distribution function is slightly different from a Maxwell-Boltzmann (MB) distribution (Ensslin, Lieu, & Biermann 1999; Blasi 2000; Dogiel 2000; Sarazin & Kempner 2000). A tail might in fact be induced in the MB distribution by the presence of MHD waves that resonate with part of the thermal electrons (Blasi 2000). This model requires an energy input comparable with the energy budget of a cluster merger and implies a substantial heating of the intracluster gas (this was shown by Blasi 2000 by solving the full Fokker-Planck equations, including Coulomb scattering). If the process lasts for too long a time (larger than a few hundred million years), the cluster is heated to a temperature well in excess of the observed ones, and the model fails. In this case the arguments presented by Petrosian (2001) apply.

The presence of tails in the MB electron distribution can be tested through observations of the Sunyaev-Zeldovich

(SZ) effect, as proposed by Blasi, Olinto, & Stebbins (2000; see Ensslin & Kaiser 2000 for a general discussion of the SZ effect including nonthermal effects). Clearly, by simply observing radio radiation and HXR radiation from clusters, it is extremely difficult, if not impossible, to discriminate among classes of models. The study of the SZ effect allows one to partly break the degeneracy. An even more powerful tool is represented by gamma-ray astronomy. Some of the models in the literature predict gamma-ray emission to some extent, while others (this is the case of nonthermal tails in the MB distribution) do not make precise predictions about the gamma-ray emission and, in fact, do not require it. Clusters of galaxies are among the targets for observations by the *GLAST* satellite. These observations will open a new window onto the nonthermal processes occurring in the intracluster gas and will allow one to understand the origin of the observed radiation at lower frequency (for a recent review, see Blasi 2003).

As stressed above, there is at present no compelling evidence in favor of any of the proposed acceleration sites for the nonthermal particles in clusters. Nevertheless, energetic events in the history of a cluster represent good candidates, and cluster mergers that build up the cluster itself hierarchically fit the description. It therefore seems reasonable to associate the existence of nonthermal particles with some process occurring during these mergers. This argument is made stronger by the fact that mergers are also thought to be responsible for the heating of the intracluster gas. Possible observational evidence for a correlation between major mergers and radio halos has recently been found by Buote (2001). In particular, the correlation exists between the radio emission at 1.4 GHz and the degree of departure from virialization in the shape of clusters, interpreted as a consequence of a recent or ongoing merger that visibly changed the dark matter distribution in the cluster core.

The shocks that are formed in the baryon components of the merging clusters are able to convert part of the gravitational energy of the system into thermal energy of the gas, as shown by direct observations (see, e.g., Markevitch, Sarazin, & Vikhlinin 1999). It has been claimed that if these shocks are strong enough, they can efficiently accelerate particles by first-order Fermi acceleration (Fujita & Sarazin 2001; Miniati et al. 2001a, 2001b; Blasi 2001). The consequences of these shocks on the nonthermal content of clusters of galaxies may be dramatic and deserve to be considered in detail. Both electrons and protons (or nuclei) are accelerated at the shock surfaces during mergers, but the dynamics of these two components is extremely different: high-energy electrons have a radiative lifetime much shorter than the age of the cluster, so that they rapidly radiate most of their energy away and eventually pile up at Lorentz factors of ~ 100 . On the other hand, protons lose only a small fraction of their energy during the lifetime of the cluster, and their diffusion time out of the cluster is even larger, so that they are stored in clusters for cosmological times (Berezinsky, Blasi, & Ptuskin 1997; Volk, Aharonian, & Breitschwerdt 1996). In other words, while for high-energy electrons only the recent merger events are important to generate nonthermal radiation that we can observe, in order to determine the proton population of a cluster (which can generate secondary electrons) we need to take into account the full history of the cluster.

In this paper we simulate merger histories of galaxy clusters and calculate the properties of the shocks generated

during the merger events and the related spectrum of particles accelerated at the shocks. We also account for the reenergization of particles preexisting within the merging clusters. We demonstrate that major mergers (mergers between clusters with comparable masses), which are supposed to be the most energetic events and are often thought to be responsible for nonthermal activity, generate shocks that are typically weak and cannot account for the spectral slopes of the observed nonthermal radiation. Shocks in small mergers are also considered, and we find that they may play an important role in generating the nonthermal radiation by primary electrons accelerated recently. As far as the proton component is concerned, the time-integrated spectra are energetically dominated by major mergers, so that the resulting spectra are very steep because of the weakness of the corresponding shocks.

Throughout the paper we assume a flat cosmology ($\Omega_0 = 1$) with $\Omega_m = 0.3$, $\Omega_\Lambda = 1 - \Omega_m = 0.7$ and a value for the Hubble constant of $70 \text{ km s}^{-1} \text{ Mpc}^{-1}$.

The paper is organized as follows: In § 2 we discuss our simulations for the reconstruction of the merger tree. In § 4 we discuss the basics of shock acceleration and reacceleration in clusters of galaxies and the physics of cosmic-ray confinement. In § 5 we describe our results, and we conclude in § 6.

2. CONSTRUCTING THE MERGER TREE OF A CLUSTER

The standard theory of structure formation predicts that larger structures are the result of the mergers of smaller structures; this hierarchical model of structure formation in the universe has been tested in several independent ways and provides a good description of the observations of the mass function of clusters of galaxies and their properties.

While a complete understanding of the process of structure formation can only be achieved by numerical N -body simulations, an efficient and analytical description can also be achieved. It represents an extremely powerful tool in that it allows one to reconstruct realizations of the merger history of a cluster with fixed mass at the present time. These analytical descriptions come in different flavors and are widely discussed in the literature. Historically, the first approach to the problem was proposed by Press & Schechter (1974, hereafter PS) and successively developed by Bond et al. (1991) and Lacey & Cole (1993, hereafter LC) among others. In the PS formalism, the differential comoving number density of clusters with mass M at cosmic time t can be written as

$$\frac{dn(M, t)}{dM} = \sqrt{\frac{2}{\pi}} \frac{\rho}{M^2} \frac{\delta_c(t)}{\sigma(M)} \left| \frac{d \ln \sigma(M)}{d \ln M} \right| \exp \left\{ -\frac{\delta_c^2(t)}{2\sigma^2(M)} \right\}. \quad (1)$$

The rate at which clusters of mass M merge at a given time t is written as a function of t and of the final mass M' (LC):

$$\begin{aligned} R(M, M', t) dM' = & \sqrt{\frac{2}{\pi}} \left| \frac{d\delta_c(t)}{dt} \right| \frac{1}{\sigma^2(M')} \left| \frac{d\sigma(M')}{dM'} \right| \\ & \times \left[1 - \frac{\sigma^2(M')}{\sigma^2(M)} \right]^{-3/2} \exp \left\{ -\frac{\delta_c^2(t)}{2} \right. \\ & \times \left. \left[\frac{1}{\sigma^2(M')} - \frac{1}{\sigma^2(M)} \right] \right\} dM', \quad (2) \end{aligned}$$

where ϱ is the present mean density of the universe, $\delta_c(t)$ is the critical density contrast linearly extrapolated to the present time for a region that collapses at time t , and $\sigma(M)$ is the current rms density fluctuation smoothed over the mass scale M . For $\sigma(M)$, we use an approximate formula proposed by Kitayama (1997), normalized by assuming a bias parameter $b = 0.9$. We adopt the expression of $\delta_c(t)$ given by Nakamura & Suto (1997). In this respect our approach is similar to that adopted by Fujita & Sarazin (2001).

Salvador-Solé, Solanes, & Manrique (1998) modified the model illustrated above by introducing a new parameter, $\Delta_m = r_{\text{crit}} = [(M' - M)/M]_{\text{crit}}$, defined as a peculiar value of the captured mass that separates the accretion events from merger events. Events in which a cluster of mass M captures a dark matter halo with mass smaller than $\Delta_m M$ are considered as continuous mass accretion, while events in which the collected mass is larger than $\Delta_m M$ are defined as mergers. The value of $\Delta_m M$ is somewhat arbitrary, but its physical meaning can be grasped in terms of modification of the potential well of a cluster, following a merger. A major merger is expected to appreciably change the dark matter distribution in the resulting cluster, while only small perturbations are expected in small mergers, which are then interpreted as events more similar to accretion than to real mergers.

Adopting this effective description of the merger and accretion events, it is easy to use the LC formalism to construct simulated merger trees for a cluster with fixed mass at the present time. Although useful from a computational point of view, this strategy of establishing a boundary between mergers and accretion events does not correspond to any real physical difference between the two types of events; therefore, in the following we will adopt the name “merger” for both regimes, provided that there is no ambiguity or risk of confusion.

In Figure 1 we plotted a possible realization of the merger tree for a cluster with present mass equal to $10^{15} M_\odot$ and

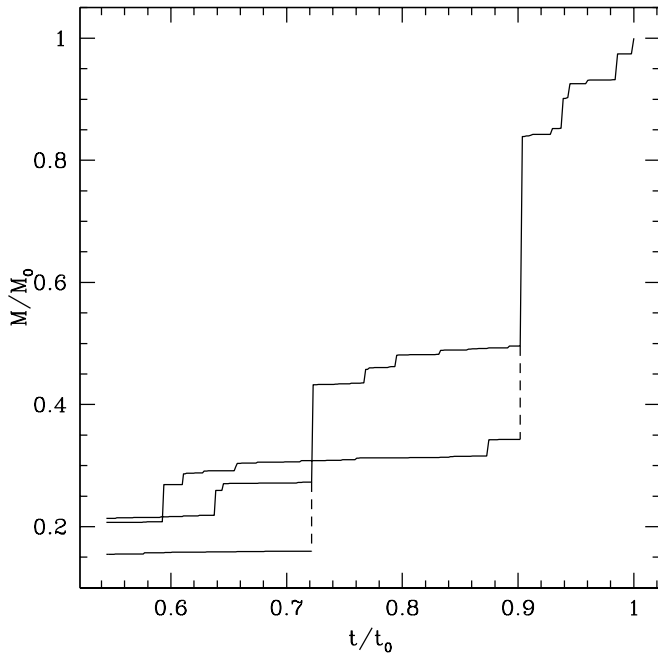


FIG. 1.—Merger history of a cluster with a present mass of $10^{15} M_\odot$. The mass (y-axis) suffers major jumps in big merger events. Time is on the x-axis.

$\Delta_m = 0.6$. The history has been followed back in time up to redshift $z = 3$. The big jumps in the cluster mass correspond to merger events, while smaller jumps correspond to what Salvador-Solé et al. (1998) defined as accretion events.

3. SHOCKS DURING CLUSTER MERGERS

During the merger of two clusters of galaxies, the baryonic component, feeling the gravitational potential created mainly by the dark matter component, is forced to move supersonically, and shock waves are generated in the intra-cluster medium.

In this section we describe in more detail the physical properties of such shocks, with special attention paid to their Mach numbers and compression factors. To this purpose, we use an approach introduced in its original version by Takizawa (1999). We assume to have two clusters, as completely virialized structures, at temperatures T_1 and T_2 and with masses M_1 and M_2 , respectively (here the masses are the total masses, dominated by the dark matter components). The virial radius of each cluster can be written as follows:

$$r_{\text{vir},i} = \left[\frac{3M_i}{4\pi\Delta_c\Omega_m\rho_{\text{cr}}(1+z_{f,i})^3} \right]^{1/3} = \left[\frac{GM_i}{100\Omega_m H_0^2(1+z_{f,i})^3} \right]^{1/3}, \quad (3)$$

where $i = 1, 2$, $\rho_{\text{cr}} = 1.88 \times 10^{-29} h^2 \text{ g cm}^{-3}$ is the current value of the critical density of the universe, $z_{f,i}$ is the redshift of formation of the cluster i , $\Delta_c = 200$ is the density contrast for the formation of the cluster, and Ω_m is the matter density fraction. In the right-hand side of the equation we used the fact that $\rho_{\text{cr}} = 3H_0^2/8\pi G$, where H_0 is the Hubble constant. The formation redshift z_f is on average a decreasing function of the mass, meaning that smaller clusters are formed at larger redshifts, consistently with the hierarchical scenario of structure formation. There are intrinsic fluctuations in the value of z_f from cluster to cluster at fixed mass because of the stochastic nature of the merger tree.

The relative velocity of the two merging clusters V_R can be easily calculated from energy conservation:

$$-\frac{GM_1M_2}{r_{\text{vir},1} + r_{\text{vir},2}} + \frac{1}{2}M_r V_r^2 = -\frac{GM_1M_2}{2R_{12}}, \quad (4)$$

where $M_r = M_1M_2/(M_1 + M_2)$ is the reduced mass and R_{12} is the turnaround radius of the system, where the two subclusters are supposed to have zero relative velocity. In fact, the final value of the relative velocity at the merger is quite insensitive to the exact initial condition of the two subclusters. In an Einstein–De Sitter cosmology this spatial scale equals twice the virial radius of the system. Therefore, using equation (3), we get

$$R_{12} = 2 \left(\frac{M_1 + M_2}{M_1} \right)^{1/3} \frac{1 + z_{f,1}}{1 + z_f} r_{\text{vir},1}. \quad (5)$$

where z_f is the formation redshift of the cluster with mass $M_1 + M_2$. This expression also remains valid in an approximate way for other cosmological models (Lahav et al.

1991). The sound speed of the cluster i is given by

$$c_{s,i}^2 = \gamma_g(\gamma_g - 1) \frac{GM_i}{2r_{\text{vir},i}},$$

where we used the virial theorem to relate the gas temperature to the mass and virial radius of the cluster. The adiabatic index of the gas is $\gamma_g = 5/3$. The Mach number of each cluster while moving in the volume of the other cluster can be written as follows:

$$\begin{aligned} \mathcal{M}_1^2 &= \frac{4(1+\eta)}{\gamma(\gamma-1)} \left[\frac{1}{1 + [(1+z_{f,1})/(1+z_{f,2})]\eta^{1/3}} \right. \\ &\quad \left. - \frac{1}{4[(1+z_{f,1})/(1+z_f)](1+\eta)^{1/3}} \right], \\ \mathcal{M}_2^2 &= \eta^{-2/3} \frac{1+z_{f,1}}{1+z_{f,2}} \mathcal{M}_1^2, \end{aligned} \quad (6)$$

where $\eta = M_2/M_1 < 1$. The procedure illustrated above can be applied to a generic couple of merging clusters, and in particular, it can be applied to a generic merger event in the history of a cluster with fixed mass at the present time. The merger history (and indeed many realizations of the history) for a cluster can be simulated as discussed in the previous section. In particular, for a cluster with mass M_0 at the present time, we simulate 500 realizations of the merger tree and calculate the Mach numbers associated with the merger events. A value $\Delta_m = 0.05$ is assumed. Note that this value is much lower than in Fujita & Sarazin (2001). This simply implies that we follow the histories of very small halos of dark matter rather than the big ones only. The results of our calculations of the Mach numbers are plotted in Figure 2.

The striking feature of this plot is that for major mergers involving clusters with comparable masses ($\eta \sim 1$), the

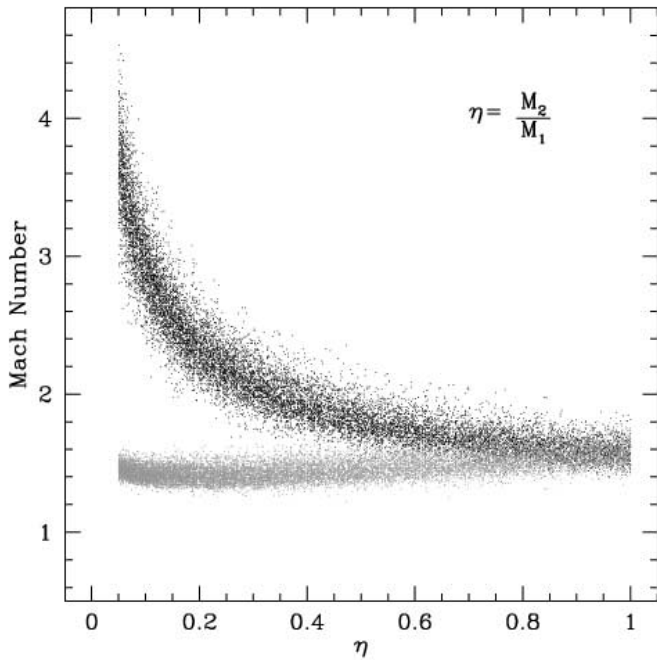


FIG. 2.—Distribution of the Mach numbers of merger-related shocks as a function of the mass ratio of the merging subclusters. The upper strip is the distribution of Mach numbers in the smaller cluster, while the lower strip refers to the bigger cluster.

Mach numbers of the shocks are of order of unity. In other words, the shocks are only moderately supersonic. In order to achieve Mach numbers of order of 3–4, one must consider mergers between clusters with very different masses ($\eta \sim 0.05$), which in the language of Salvador-Solé et al. (1998) and Fujita & Sarazin (2001) would not be considered mergers but rather continuous accretion. These events are the only ones that produce strong shocks, and this is of crucial importance for the acceleration of suprathermal particles, as discussed below.

In Figure 3 we plotted a histogram of the frequency of shocks with given Mach number. It is easy to see that the greatest part of the merger shocks are weak, with a peak in Mach number at about 1.4. This result is in some contradiction to the Mach number distribution found by Miniati et al. (2000), which is a bimodal distribution with one peak at Mach numbers of ~ 1000 and one at Mach numbers of ~ 5 . While the former peak cannot be obtained within our approach, because it is caused by shocks in the cold outskirts of clusters, not directly related to merger events, the latter shocks should be the same as those described in our paper. In fact, they are located, according to Miniati et al. (2000), within $0.5 h^{-1}$ Mpc of the cluster center, namely, in the virialized region, so that the arguments presented here do apply. It is worth noticing in passing that the simulations of Miniati et al. (2000) have an intrinsic cutoff at Mach numbers smaller than $\sqrt{3}$, so that the peak we find at 1.5 is out of the available range. It is also worth noticing that the spatial resolution achieved in these simulations is $0.315 h^{-1}$ Mpc, very close to the size of the region ($0.5 h^{-1}$ Mpc) where the shocks need to be identified.

On the other hand, the simple method introduced in our paper in order to evaluate the Mach number of merger-related shocks suffers from the limitation of being applicable only to binary mergers. The cases in which a cluster is merging with another cluster in a deeper gravitational potential well generated by a collection of nearby structures cannot be treated in the context of this method. The occurrence of

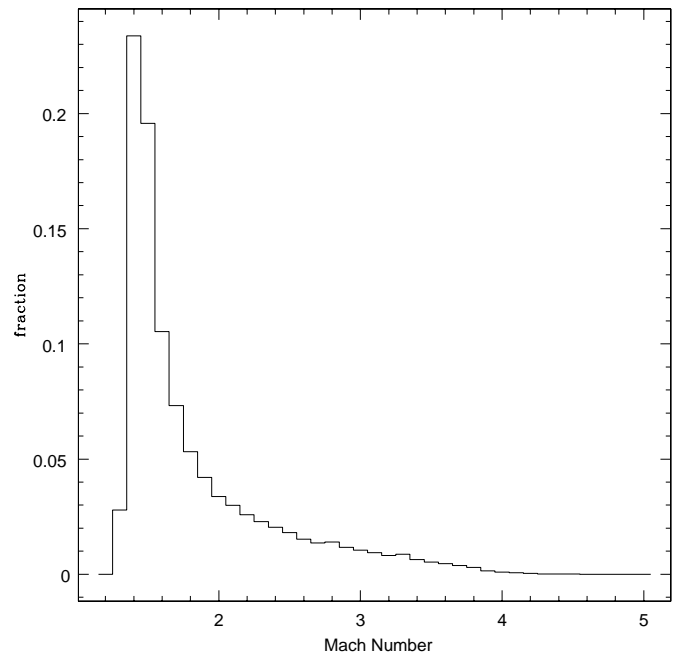


FIG. 3.—Distribution of the Mach numbers of merger-related shocks

these events may induce fluctuations around the mean Mach number that might be larger than those considered here. We discuss this limitation more quantitatively in § 5.

The presence of the shocks at very large Mach numbers in the intergalactic medium well outside virialized structures like clusters of galaxies can be expected simply on the basis of the propagation of shocks moving with speed typically 10^8 cm s^{-1} in a cold medium, with, say, $T \sim 10^4 \text{ K}$. These shocks can accelerate particles efficiently; if these particles are electrons, their radiation is expected to be concentrated around the shocks and well outside the intracluster medium. If the accelerated particles are protons, they are expected to be advected inside the cluster by the accretion flow, where their inelastic collisions can generate secondary radiation (S. Gabici & P. Blasi 2003, in preparation).

Observationally, the strength of merger-related shocks has been measured from high-resolution X-ray images that allow one to evaluate the temperatures on the two sides of a shock. One instance is provided by Cygnus A ($z = 0.057$), where two subclusters with comparable masses ($\eta \sim 1$) are merging. *ASCA* observations of this cluster have been used by Markevitch et al. (1999) to determine the temperature upstream ($T_1 = 4 \pm 1 \text{ keV}$) and downstream ($T_2 = 8_{-1}^{+2} \text{ keV}$) of the shock, so that the compression factor r at the same shock can be determined from the Rankine-Hugoniot relations:

$$\frac{1}{r} = \left[4 \left(\frac{T_2}{T_1} - 1 \right)^2 + \frac{T_2}{T_1} \right]^{1/2} - 2 \left(\frac{T_2}{T_1} - 1 \right). \quad (7)$$

Numerically, we obtain $r \sim 2.2$ – 2.4 , corresponding to a Mach number $\mathcal{M} \sim 2$, roughly consistent with our predictions in Figure 2. Other cases of current merger events provide further examples of moderately supersonic relative motion of the merging clusters (Markevitch & Vikhlinin 2001; Markevitch et al. 2002). None of the observed shocks seem to have Mach numbers ~ 5 , which appears to be in agreement with our findings. If the peak in Mach numbers were at ~ 5 , it would be statistically unfavorable to observe only Mach numbers smaller than this value.

4. ACCELERATION AND CONFINEMENT OF COSMIC RAYS

Relativistic particles can be accelerated at strong shocks by diffusive (first-order) Fermi acceleration (Fermi 1949; Blandford & Eichler 1987). This mechanism has been invoked several times as the ideal acceleration process in clusters of galaxies that are or have been involved in a merger event (Blasi 2001; Fujita & Sarazin 2001). In § 4.1 we briefly summarize the basic physics of shock acceleration since it is instrumental to understand whether merger-related shock waves can indeed play a role for the acceleration of the relativistic particles responsible for the observed nonthermal radiation from clusters of galaxies. In § 4.2 we summarize the findings of Berezhinsky et al. (1997) on the confinement of cosmic rays in clusters of galaxies for cosmological timescales. In § 4.3 we briefly explain how to extend the formalism of shock acceleration to the reenergization of the particles confined in the cluster volume.

4.1. Shock Acceleration

A shock with compression factor r and Mach number \mathcal{M} can accelerate particles to a power law in momentum $f(p) \propto p^{-\alpha}$, with slope α related to the Mach number and compression factor by the following expression:

$$\alpha = \frac{r+2}{r-1} = 2 \frac{\mathcal{M}^2 + 1}{\mathcal{M}^2 - 1}. \quad (8)$$

The acceleration occurs diffusively, in that particles scatter back and forth across the shock, gaining at each crossing and recrossing an amount of energy proportional to the energy of the particle itself, $\Delta E/E \sim V/c$, where V is the speed of the shock and c is the speed of light. The distribution function of the accelerated particles is normalized here by $\int_{p_{\min}}^{p_{\max}} dp E(p) f(p) = \eta_{\text{shock}} \rho u^2$, where $E(p) = (p^2 + m^2)^{1/2}$, m is the mass of the accelerated particles, η_{shock} is an efficiency of acceleration, and ρ and u are the density and speed, respectively, of the fluid crossing the shock surface. The minimum and maximum momenta (p_{\min} and p_{\max}) of the accelerated particles are determined by the properties of the shock. In particular, p_{\max} is the result of the balance between the acceleration rate and either the energy loss rate or the rate of escape from the acceleration region. Less clear is how to evaluate p_{\min} ; the minimum momentum of the particles involved in the acceleration process depends on the microphysics of the shock, which is very poorly known. Fortunately, most of the physical observables usually depend very weakly on p_{\min} .

The basic points introduced above can be simply applied to the case of shocks that originated in cluster mergers, where the approximate values of the parameters are known. In the following, we use these parameters to estimate the maximum energies attainable for electrons and protons as accelerated particles. The acceleration time, as a function of the particle energy E , can be written as

$$\tau_{\text{acc}}(E) = \frac{3}{u_1 - u_2} D(E) \left(\frac{1}{u_1} + \frac{1}{u_2} \right) = \frac{3D(E)r(r+1)}{v^2(r-1)}, \quad (9)$$

valid for any choice of the diffusion coefficient $D(E)$, for which we consider two possible models. First, we use the expression proposed in Blasi & Colafrancesco (1999):

$$D(E) = 2.3 \times 10^{29} B_{\mu}^{-1/3} L_{20}^{2/3} E(\text{GeV})^{1/3} \text{ cm}^2 \text{ s}^{-1}, \quad (10)$$

where B_{μ} is the magnetic field in microgauss and L_{20} is the largest scale in the magnetic field power spectrum in units of 20 kpc. Here we assumed that the magnetic field is described by a Kolmogorov power spectrum.

In this case the acceleration time becomes

$$\tau_{\text{acc}}(E) \approx 6.9 \times 10^{13} B_{\mu}^{-1/3} L_{20}^{2/3} E(\text{GeV})^{1/3} v_8^{-2} g(r) \text{ s}, \quad (11)$$

where $v_8 = v/10^8 \text{ cm s}^{-1}$, $g(r) = r(r+1)/(r-1)$, and $v = u_1$.

For electrons, energy losses are dominated by ICS off the photons of the cosmic microwave background, provided that the magnetic field is smaller than $\sim 3 \mu\text{G}$. The maximum energy of accelerated electrons is obtained by requiring $\tau_{\text{acc}} < \tau_{\text{loss}}$:

$$E_{\text{max}}^e \approx 118 L_{20}^{-1/2} B_{\mu}^{1/4} v_8^{3/2} g(r)^{-3/4} \text{ GeV}. \quad (12)$$

The relation between the compression ratio r and the Mach

number is

$$r = \frac{8/3 \mathcal{M}^2}{2/3 \mathcal{M}^2 + 2}, \quad (13)$$

valid for an ideal monoatomic gas. Here \mathcal{M} is the Mach number of the unshocked gas, moving with speed v_8 .

For protons, energy losses are usually not relevant, and the maximum energy is clearly determined by the finite time duration of the merger event. Therefore, the maximum energy for protons will be defined by the condition $\tau_{\text{acc}} < t_{\text{merger}}$, which gives

$$E_{\text{max}}^p \approx 9 \times 10^7 L_{20}^{-2} B_{\mu} v_8^6 g(r)^{-1/2} \text{ GeV} \quad (14)$$

for $t_{\text{merger}} \sim 10^9$ yr. As a second possibility for the diffusion coefficient, we assume Bohm diffusion, well motivated for the case of strong turbulence. In this case

$$D(E) = 3.3 \times 10^{22} \frac{E}{B_{\mu}} \text{ cm}^2 \text{ s}^{-1}. \quad (15)$$

For electrons, we obtain

$$E_{\text{max}}^e \approx 6.3 \times 10^4 B_{\mu}^{1/2} v_8 g(r)^{-1/2} \text{ GeV}, \quad (16)$$

while for protons, we obtain

$$E_{\text{max}}^p \approx 3 \times 10^9 B_{\mu} v_8^2 g(r)^{-1} \text{ GeV}. \quad (17)$$

If E_{max}^p becomes larger than $\sim 10^{10}$ GeV, energy losses due to proton pair production and photopion production on the photons of the microwave background become important and limit the maximum energy to less than a few times 10^{10} GeV (Kang, Rachen, & Biermann 1997).

The relative abundance of electrons and protons at injection is an unknown quantity. Theoretically, there are plausibility arguments for having a small e/p ratio, related to the microphysics of shock acceleration: Protons resonate with Alfvén waves on a wide range of momenta, so that they can be efficiently extracted from the thermal distribution and injected into the acceleration engine. For electrons, this is much harder. Low-energy electrons do not interact with Alfvén waves, and some other modes need to be excited (e.g., whistlers) and sustained against their strong damping. A detailed discussion of the electron injection at nonrelativistic shocks can be found in McClements et al. (1997) and Levinson (1994 and references therein).

Another issue that contributes to the suppression of the injection of the electron component in a shock is the finite thickness of the shock, comparable with the Larmor radius of thermal protons (Bell 1978a, 1978b). Electrons can be injected in the shock accelerator only if their Larmor radius is larger than the thickness of the shock. For a proton temperature of ~ 8 keV, only electrons with energy larger than ~ 5 – 10 MeV can be injected in the acceleration box. This energy is much larger than the typical electron temperature in the intracluster medium. The value of 5 MeV can be adopted as a sort of low-energy cutoff in the injection spectrum of electrons.

4.2. Confinement of Accelerated Particles

It was first realized by Berezhinsky et al. (1997) and Volk et al. (1996) that the bulk of the hadronic cosmic rays accel-

ated or injected in clusters of galaxies remain diffusively confined within the cluster volume for cosmological times. The maximum energy for which the confinement is effective is a strong function of the assumed diffusion coefficient, being the highest for the case of Bohm diffusion. For this case, for our purposes we can assume a complete confinement. In cases that might be more realistic, for instance, for a Kolmogorov spectrum of magnetic fluctuations, the confinement may be limited to particles with energy up to a few TeV.

For the energies at which the confinement is effective, the energy density in cosmic rays increases with time because of the pile up of particles injected during the cluster history. In particular this accumulation occurs at each merger event if the merger-related shocks are strong enough. This process may result in a sufficient accumulation of cosmic-ray protons to induce detectable fluxes of gamma radiation through pion decay (see Blasi 2003 for a recent review).

For high-energy electrons, the processes that affect the propagation the most are energy losses, so that the discussion on confinement does not apply. On the other hand, the confined protons induce a secondary population of electron-positron pairs due to the decay of charged pions generated in inelastic collisions of relativistic protons with the thermal gas. These pairs are responsible for radio radiation through synchrotron emission and for X-rays due to ICS. Moreover, gamma radiation is also generated through ICS and bremsstrahlung emission of these secondary pairs.

Low-energy electrons ($\gamma \sim 100$) lose energy slowly and can be piled up and confined for a few billion years and eventually reenergized by shocks related to successive merger events.

4.3. Reacceleration of Confined Relativistic Particles

Shocks formed during a merger not only accelerate new particles from the thermal bath but also reenergize particles confined in the cluster from either previous mergers or additional sources of cosmic rays. Low-energy electrons and relativistic hadrons are affected by the reacceleration.

Assuming that the spectrum of particles confined within the cluster is $n(p)$ and that the merger shock has a compression factor r , the spectrum of the reaccelerated particles can be easily calculated. In fact, particles with initial momentum between p and $p + dp$ are $n(p)dp$, and they are reprocessed by the shock into the spectrum $df(p')$, which can be calculated by standard shock acceleration theory:

$$df(p') = dA \left(\frac{p'}{p} \right)^{-\alpha}, \quad \alpha = \frac{r+2}{r-1} \quad (18)$$

and

$$\int_p^{\infty} dp' df(p') = n(p)dp \rightarrow dA = (\alpha - 1)n(p) \frac{dp}{p}, \quad (19)$$

where we assume $\alpha > 1$ and $p_{\text{max}} \rightarrow \infty$. The spectrum of all the reaccelerated particles is then

$$f(p') = \int_{p_{\text{min}}}^{p'} \frac{dp}{p} (\alpha - 1)n(p) \left(\frac{p'}{p} \right)^{-\alpha}. \quad (20)$$

If the initial spectrum of the particles is a power law

$n(p) = n_0(p/p_{\min})^{-\beta}$, then equation (20) gives

$$f(p') = \frac{\alpha - 1}{\alpha - \beta} n_0 \left(\frac{p'}{p_{\min}} \right)^{-\alpha} \left[\left(\frac{p'}{p_{\min}} \right)^{\alpha - \beta} - 1 \right] \quad (21)$$

for $\alpha > \beta$ (a similar expression is obtained for $\beta > \alpha$) and

$$f(p') = (\alpha - 1) n_0 \left(\frac{p'}{p_{\min}} \right)^{-\alpha} \ln \left(\frac{p'}{p_{\min}} \right) \quad (22)$$

for $\alpha = \beta$. A typical effect of reacceleration is to generate particle spectra that are flatter than the spectrum of the seed particles. Moreover, at each reacceleration step, the total energy in accelerated particles can be substantially increased if the shocks are sufficiently strong. Note that equation (20) holds for an arbitrary spectrum of the preexisting particles.

Low-energy electrons, which may also be confined for a few billion years with no appreciable energy loss within the clusters, may also be reenergized by the passage of merger shocks, so that for the duration of the merger they can reach the relativistic energies required to produce the nonthermal radiation observed in the radio and X-ray bands. Strong shocks, with Mach numbers of order of ~ 3 – 4 , are needed in order to explain observations.

5. SIMULATED SHOCKS AND SPECTRA OF NONTHERMAL PARTICLES

The technique described in § 2 allows us to simulate merger trees of a cluster and evaluate the physical properties of the shock waves generated at each merger of subclusters, as discussed in § 3. While the merger tree is constructed moving backward in time, starting with a cluster of given mass at the present time, the shock properties and particle acceleration are reconstructed by moving forward in time and accounting for the mergers of all the substructures generated during the first step of the simulation (backward in time).

Each merger here is assumed to be a two-body event. This is clearly increasingly less true for large mass differences between the merging subclusters because it may happen that more subclusters with small masses can *accrete* onto the big cluster at approximately the same time. In other words, the merger between two clusters may occur in the deeper gravitational potential well created by nearby structures. In this case, the relative velocity between the two clusters and also the related shock Mach numbers may be larger (or smaller) than those estimated in § 3. Although a rigorous evaluation of the probability of occurrence of this kind of situation cannot be carried out in the context of our simple approach, convincing arguments can be provided to support the results discussed in § 3; let us assume that our two clusters, with mass M_1 and M_2 , are merging in a volume of average size R_{sm} , where the overdensity is $1 + \delta$ ($\delta = 0$ corresponds to matter density equal to the mean value). Clearly, the overdense region must contain more mass than that associated with the two clusters; therefore, for a top-hat overdensity at $z = 0$, we can write

$$\frac{4}{3} \pi R_{\text{sm}}^3 \rho_{\text{cr}} \Omega_m (1 + \delta) = \xi (M_1 + M_2), \quad (23)$$

where $\xi > 1$ is a measure of the mass in the overdense region in excess of $M_1 + M_2$. In numbers, using $\Omega_m = 0.3$, this

condition becomes

$$1 + \delta = 2\xi M_{15} R_{10}^{-3}, \quad (24)$$

where M_{15} is $M_1 + M_2$ in units of $10^{15} M_{\odot}$ and $R_{\text{sm}} = 10 \text{ Mpc } R_{10} h^{-1}$.

If the clusters are affected by the potential well of an overdense region with total mass M_{tot} , the maximum relative speed that they can acquire is $v_{\text{max}} \approx 2(GM_{\text{tot}}/R_{\text{sm}})^{1/2}$. Note that this would be the relative speed of the two clusters if they merged at the center of the overdense region and with a head-on collision; therefore, any other (more likely) configuration would imply a relative velocity smaller than v_{max} . In particular, the presence of the local overdensity might even cause a slow down of the two merging clusters rather than a larger relative velocity. In numbers, this is

$$v_{\text{max}} = 1.1 \times 10^8 \xi^{1/2} M_{15}^{1/2} R_{10}^{-1/2} \text{ cm s}^{-1}.$$

Using the usual expression for the sound speed in a cluster with mass M_i , we also get

$$c_s = 8.8 \times 10^7 M_{i,15}^{1/3} \text{ cm s}^{-1}.$$

Therefore, the maximum Mach number that can be achieved in the i th cluster is

$$\mathcal{M}_{i,\text{max}} = 1.25 \xi^{1/2} R_{10}^{-1/2} M_{15}^{1/2} M_{i,15}^{-1/3}. \quad (25)$$

As stressed in the previous sections, the Mach numbers that may be relevant for particle acceleration are $\mathcal{M} > 3$, which implies the following condition on ξ :

$$\xi > 5.8 M_{15}^{-1} M_{i,15}^{2/3} R_{10}, \quad (26)$$

which when introduced in equation (24) gives

$$1 + \delta > 11.6 R_{10}^{-2} M_{i,15}^{2/3}. \quad (27)$$

Similar results may be obtained using the velocity distribution of dark matter halos as calculated in semianalytical models (Sheth & Diaferio 2001) and transforming this distribution into a pairwise velocity distribution by adopting a suitable recipe.

The probability to have an overdensity $1 + \delta$ in a region of size R_{sm} has the functional shape of a lognormal distribution, as calculated by Kayo, Taruya, & Suto (2001). Equation (27) gives the overdensity $1 + \delta$ necessary for a cluster of mass M_i to achieve a Mach number of at least 3 in the collision with another cluster in the same overdense region. In Table 1 we report the probabilities $P(\delta)$ as a function of M_i , evaluated following Kayo et al. (2001) for different sizes of the overdense region.

These numbers must be interpreted as upper limits to the probability that a cluster of mass M_i develops a merger shock with Mach number larger than 3 since the probabilities refer to the configuration in which the relative velocity between the two clusters is maximized. For rich clusters, with masses larger than $5 \times 10^{14} M_{\odot}$ (corresponding to X-ray luminosities $L_X > 4 \times 10^{44} \text{ ergs s}^{-1}$), the probability that the presence of a local overdensity may generate Mach numbers relevant for the nonthermal activity has been estimated to be $\sim 10^{-3}$ or smaller, suggesting that our two-body approximation is reasonable, in particular for the massive clusters that are typically observed to have nonthermal activity. For smaller clusters, the probabilities become

TABLE 1
PROBABILITIES $P(\delta)$ AS A FUNCTION OF M_i FOR
DIFFERENT SIZES OF THE OVERDENSE REGION

$M_{i,15}$	R_{10}	$(1 + \delta)$	$P(\delta)$
1.....	0.8	18.1	7×10^{-5}
	1	11.6	9×10^{-5}
	1.2	8.1	10^{-4}
0.5.....	0.8	11.4	5×10^{-4}
	1	7.3	10^{-3}
	1.2	5.1	2×10^{-3}
0.1.....	0.8	3.9	2×10^{-2}
	1	2.5	5×10^{-2}
	1.2	1.7	0.12

higher, indicating that the distribution of Mach numbers might have a larger spread compared with that illustrated in Figure 2. Note, however, that for small clusters, even the two-body approximation gives relatively high Mach numbers, provided that the merger occurs with a bigger cluster, simply as a result of a lower temperature and a correspondingly lower sound speed.

Motivated by this argument, in the following we will continue to consider only binary mergers.

For each of these binary mergers, we evaluate the duration of the merger and the relative volumes that take part in it.

A prescription on how to define these two quantities is required since they affect the amount of energy injected in the cluster in the form of relativistic particles. Acceleration occurs at each one of the two shocks formed as a result of the merger. Once the relative velocity is calculated from equation (4), the duration of the merger event is defined as

$$\tau_{\text{mer}} \approx \frac{r_{\text{vir},1}}{V_r},$$

where $r_{\text{vir},1}$ is defined as the virial radius of the bigger cluster. The geometry of the merger is schematized in Figure 4.

It is extremely important to keep in mind that the radiation from electrons directly accelerated at a shock is, in first

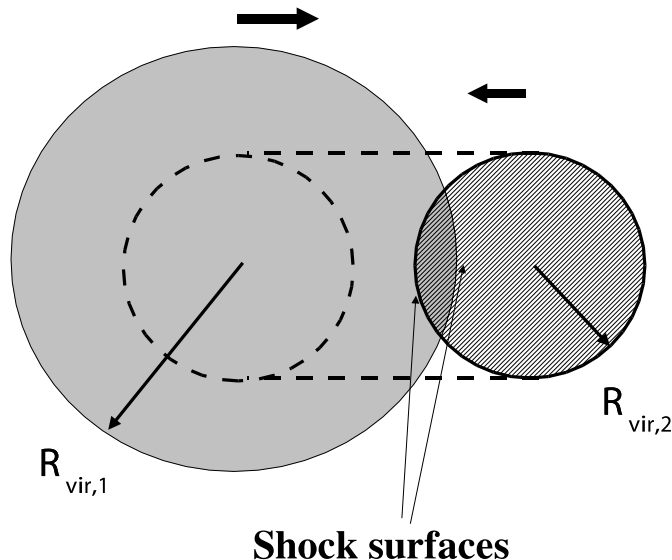


FIG. 4.—Geometry of the merger between two subclusters

approximation, solely dominated by the last merger events that the cluster suffered; on the other hand, for protons and the consequent secondary products, it is mandatory to study the full history of the cluster and account for all the shocks that traversed the cluster volume. Both acceleration of new particles and reenergization of previously accelerated particles need to be taken into account, as explained in § 4.

Observations may be explained by a population of electrons (primaries or secondaries) injected in the cluster with a power-law spectrum having a slope around 2.3–2.4 (see, e.g., Blasi 2001). In the discussion below we will refer exclusively to injection spectra, without explicitly accounting for the obvious steepening by one power in energy in the equilibrium spectrum of the radiating electrons (energy losses are dominated by ICS and synchrotron emission in the energy range of interest). In other words, if the injection spectrum of electrons (as primaries or as secondary products of hadronic interactions) is (locally) a power law with slope 2.3–2.4, the corresponding equilibrium spectra will have local slope 3.3–3.4.

In the following we distinguish the two cases of primary electrons (directly accelerated at the shocks) and secondary electrons, whose spectrum at energies above a few GeV approximately reproduces the spectrum of the parent protons. We start with the case of secondary electrons, concentrating our attention on the spectrum of the accelerated protons. We stress again that merger-related shocks accelerate *new* protons and reaccelerate protons that were already confined in the parent clusters from previous times. The efficiency for particle acceleration at each shock is taken as a constant equal to 10%. For simplicity, we assume that the accelerated particles are all confined in the cluster volume, although this may not be true at the highest energies for large diffusion coefficients. It seems, however, a good approximation for protons with the energies that we are interested in. The spectra that result from our calculations are plotted in Figure 5. These curves are obtained averaging

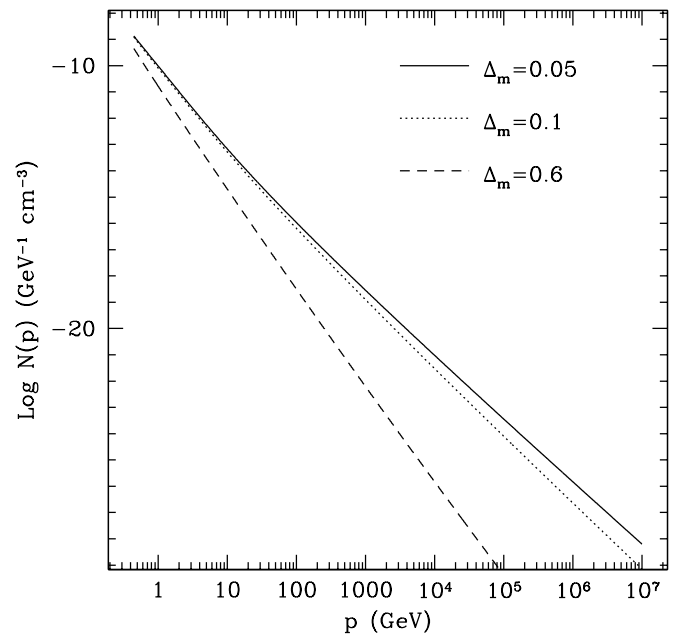


FIG. 5.—Time-integrated average proton spectra resulting from all the mergers in a cluster. The three curves are obtained for $\Delta_m = 0.05$ (solid line), $\Delta_m = 0.1$ (dotted line), and $\Delta_m = 0.6$ (dashed line).

the spectra of 500 clusters, each one followed in its merger history back in time to redshift $z = 3$. We consider the three cases $\Delta_m = 0.6$ (dashed line), $\Delta_m = 0.1$ (dotted line), and $\Delta_m = 0.05$ (solid line). It is clear that at high energy it is crucial to account for small mergers since they are responsible for flatter spectra. In fact, the flatter regions are also due to some level of reacceleration of preexisting protons, confined in the intracluster volume. If only major mergers are considered ($\Delta_m = 0.6$), the resulting spectrum is too steep to be of any relevance for the generation of the observed nonthermal radiation.

In Figure 6 we plot the distribution of spectral slopes (α in eq. [8]) for different choices of the threshold in mass ratio for mergers. Since the spectra are not power laws (see Fig. 5), it is convenient to plot the slopes at fixed energy, say 10 GeV (it is worth recalling that protons with this energy typically generate electrons of few GeV, which are the ones relevant for the production of radio halos). When major mergers are considered ($\Delta_m = 0.6$), the typical slopes of the spectra of accelerated particles peak around 4.4, too steep to be relevant for nonthermal radiation in clusters. When mergers between clusters with very different masses are considered, the situation improves, but still, even for $\Delta_m = 0.05$, the spectra remain too steep. An important point is that flat spectra, if any, are not obtained in major mergers but rather in those mergers that according to Fujita & Sarazin (2001) qualify as *accretion* events. Shocks related to major mergers are not strong enough to account for the observed spectra. The spread in the values of α in Figure 6 reflects the fluctuations in the Mach numbers in Figure 2, because of the distribution of formation redshifts in the simulation and to the stochasticity of the merger tree. Even accounting for these fluctuations, the strength of the shocks appears to be insufficient to generate the required spectra of accelerated particles.

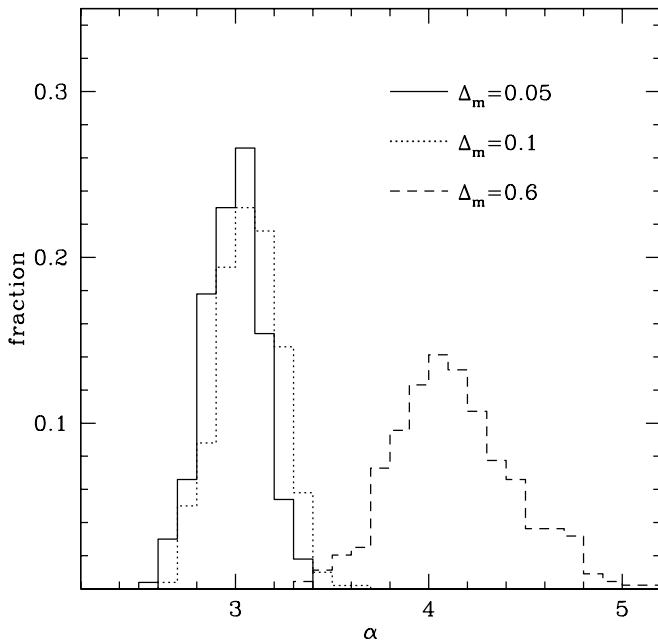


FIG. 6.—Slope of the time-integrated proton spectra at energy 10 GeV resulting from all the mergers in a cluster. The three curves are obtained for $\Delta_m = 0.05$ (solid line), $\Delta_m = 0.1$ (dotted line), and $\Delta_m = 0.6$ (dashed line).

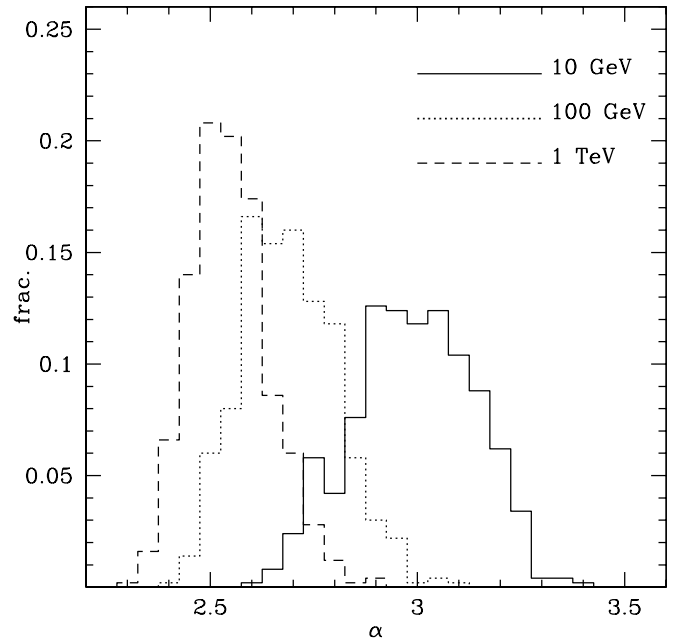


FIG. 7.—Same as Fig. 6, but for $\Delta_m = 0.05$ at different proton energies: 10 GeV (solid line), 100 GeV (dotted line), and 1 TeV (dashed line).

In Figure 7 we also plot the slope of the proton spectrum for $\Delta_m = 0.05$ at three energies: 10 GeV (solid line), 100 GeV (dotted line), and 1 TeV (dashed line). It is clear that the spectrum flattens at high energies, which is again in some disagreement with observations of radio halos, which seem to suggest a steepening of the radio spectrum toward its higher frequency end.

We now consider the acceleration of primary electrons as responsible for nonthermal radiation in clusters of galaxies. In this case, only recent mergers, occurring within about one billion years, may be related to the observed radiation, because of the short lifetimes of relativistic electrons. Therefore, we simulate the merger tree of clusters with fixed present mass, limiting the simulations to one billion years far into the past. In fact, even one billion years is a time appreciably longer than the time for losses of relativistic electrons, so that our predictions have to be considered as optimistic. Mergers and related shocks have been treated as discussed in the previous sections.

Of the 500 clusters with mass $10^{15} M_\odot$ for which we simulated the merger tree, about 30% suffered for a merger during the last billion years. In Figure 8 we plotted the Mach numbers of the shocks generated in the clusters that suffered at least one merger (actually, it is rare to have more than one merger during the last billion years). The dashed line represents the value of the Mach number that would correspond to a slope of the accelerated electrons equal to 2.4, required to explain observations. Only 20% of the shocks have Mach numbers fulfilling this condition, so that in the end, about 6% of the 500 simulated $10^{15} M_\odot$ clusters of galaxies have suffered a merger that may have generated nonthermal activity with a Coma-like spectrum.

6. CONCLUSIONS

We investigated the possibility that the nonthermal activity observed from some clusters of galaxies may originate

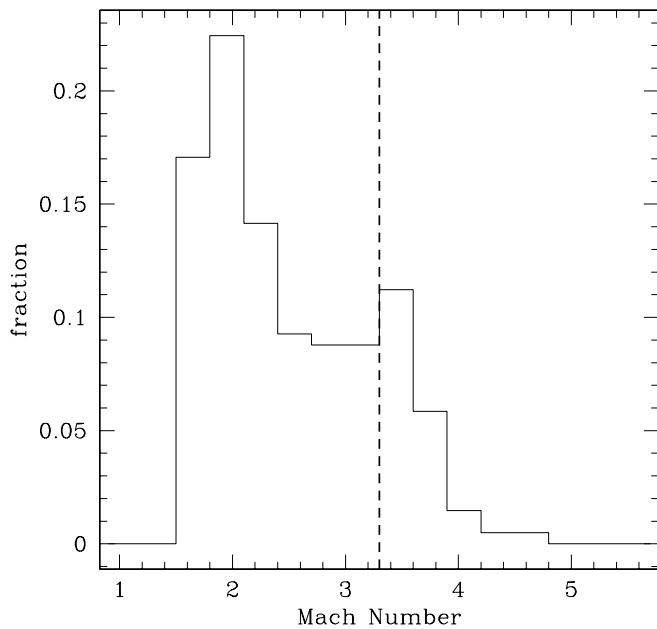


FIG. 8.—Distribution of Mach numbers for the mergers occurred in the last one billion years for a cluster with present mass $10^{15} M_{\odot}$. The dashed line indicates the Mach number that corresponds to shocks able to accelerate electrons with a spectrum $E^{-2.4}$. The histogram is obtained averaging over 500 clusters.

through radiative losses of electrons either accelerated at shocks during cluster mergers or produced as secondary products of the inelastic collisions of protons, in turn accelerated at the same merger shocks.

While the spectrum of protons at any time is the result of all the merger history of a cluster, because of cosmic-ray confinement (Berezinsky et al. 1997; Volk et al. 1996), primary electrons that are able to radiate radio or X-ray photons at present need to be accelerated in very recent times, so that only the last mergers are relevant (Fujita & Sarazin 2001).

The merger history of clusters can be simulated by using a PS approach, which allows one to obtain, for each merger event, the mass of the subclusters. In the reasonable assumption of binary mergers, it is also easy to calculate the relative velocity of the two merging clusters and, if clusters are assumed to be virialized structures, also the Mach numbers of the two approaching subclusters. Once the Mach numbers are known, it is possible to calculate the spectra of the particles accelerated by first-order Fermi acceleration.

We discussed separately the case of secondary and primary electrons. The secondary electrons, generated in pp scattering, have a spectrum that approximately reproduces the spectrum of the parent protons (because of Feynman scaling for the cross section). The spectrum of the protons is calculated by taking into account the acceleration process at each merger and the reacceleration of protons confined in the merging clusters. The spectrum at the present time is the result of these processes along the all history of the cluster. The spectra that we obtained from our calculations are typically steeper than those required to explain the observed nonthermal radiation. This result is the consequence of the weakness of the shocks associated with major mergers, where the relative motion of the two subclusters occurs at

almost free-fall velocity, which implies Mach numbers only slightly larger than unity. Minor mergers produce stronger shocks, but they are energetically subdominant.

Mach numbers larger than those calculated here may be achieved if the merger event occurs in an overdense region, where the infall motion of the two clusters may be dominated by the gravitational well of the surrounding matter rather than by the mutual interaction between the two clusters. This kind of situation can indeed either increase or decrease the Mach numbers compared with the binary case. In § 5 we have found that in order to obtain Mach numbers larger than ~ 3 the overdensity must be such that for rich clusters (mass larger than $5 \times 10^{14} M_{\odot}$) the probability of sitting in such a potential is pretty slim, and the binary merger model should represent an accurate description of reality, in a statistical sense.

As stressed above, primary electrons can generate observable nonthermal radiation only if accelerated in recent mergers that occurred less than 10^9 yr ago. Our simulations of 500 clusters with mass $10^{15} M_{\odot}$ show that only $\sim 6\%$ of them seem to have nonthermal activity with the same spectral features observed in the Coma Cluster. This number should be compared with the statistics of radio halos (Feretti et al. 2000), which seem to suggest that $\sim 30\%$ of the clusters with X-ray luminosity larger than $10^{45} \text{ ergs s}^{-1}$ have such radio halos. This comparison should, however, be taken with caution. In fact, if the radio halos found by Feretti et al. (2000) have steep spectra, then our statistics increase appreciably, and the disagreement may be attenuated. Unfortunately, the spectrum is not available for all radio halos. A more detailed analysis of recent mergers accounting in detail for the time-dependent electron losses is being currently carried out (S. Gabici & P. Blasi 2003, in preparation).

We can summarize our conclusions as follows:

1. The diffuse nonthermal activity should not be directly associated with protons accelerated at merger shocks within the cluster volume.
2. The nonthermal activity should not correlate directly with major cluster mergers, unless the turbulence induced by mergers is responsible for particle acceleration; if a correlation is confirmed between radio halos and clusters that suffered major mergers, as seems to emerge from the analysis of Buote et al. (2001), then the natural conclusion is that the nonthermal particles are not accelerated at shocks but rather energized by other processes, possibly related to resonant wave-particle interactions.
3. If electrons directly accelerated at merger shocks are the sources of radio halos and HXR emission, then only about 6% of the clusters with mass $10^{15} M_{\odot}$ are expected to have such nonthermal activity (note that even in these cases the acceleration is not expected to occur at shocks formed during major mergers).

We are grateful to G. Brunetti and A. Diaferio for many instructive discussions on the topics of nonthermal radiation in clusters of galaxies and velocity dispersions of clusters in overdense regions, respectively. We want also to thank the anonymous referee for his comments that helped us to improve the paper.

REFERENCES

- Bell, A. R. 1978a, *MNRAS*, 182, 147
 ———. 1978b, *MNRAS*, 182, 443
 Berezhinsky, V. S., Blasi, P., & Ptuskin, V. S. 1997, *ApJ*, 487, 529
 Blandford, R., & Eichler, D. 1987, *Phys. Rep.*, 154, 1
 Blasi, P. 2000, *ApJ*, 532, L9
 ———. 2001, *Astropart. Phys.*, 15, 223
 ———. 2003, in *Matter and Energy in Clusters of Galaxies*, ed. S. Bowyer & C.-Y. Hwang (San Francisco: ASP), in press
 Blasi, P., & Colafrancesco, S. 1999, *Astropart. Phys.*, 12, 169
 Blasi, P., Olinto, A. V., & Stebbins, A. 2000, *ApJ*, 535, L71
 Bond, J. R., Cole, S., Efstathiou, G., & Kaiser, N. 1991, *ApJ*, 379, 440
 Brunetti, G., Setti, G., Feretti, L., & Giovannini, G. 2001, *MNRAS*, 320, 365
 Buote, D. A. 2001, *ApJ*, 553, L15
 Clarke, T. E., Kronberg, P. P., & Böhringer, H. 1999, in *Diffuse Thermal and Relativistic Plasma in Galaxy Clusters*, ed. H. Böhringer, L. Feretti, & P. Schuecke (Garching: MPE), 82
 Colafrancesco, S., & Blasi, P. 1998, *Astropart. Phys.*, 9, 227
 Dennison, B. 1980, *ApJ*, 239, L93
 Dogiel, V. A. 2000, *A&A*, 357, 66
 Dolag, K., & Ensslin, T. 2000, *A&A*, 362, 151
 Eilek, J. A. 1999, in *Diffuse Thermal and Relativistic Plasma in Galaxy Clusters*, ed. H. Böhringer, L. Feretti, & P. Schuecker (Garching: MPE), 71
 Ensslin, T. A., & Kaiser, C. R. 2000, *A&A*, 360, 417
 Ensslin, T. A., Lieu, R., & Biermann, P. L. 1999, *A&A*, 344, 409
 Feretti, L., Brunetti, G., Giovannini, G., Govoni, F., & Setti, G. 2000, in 2000 IAP Conf.: Constructing the Universe with Clusters of Galaxies, ed. F. Durret & D. Gerbal (Paris: IAP), 37
 Fermi, E. 1949, *Phys. Rev.*, 75, 1169
 Fujita, Y., & Sarazin, C. L. 2001, *ApJ*, 563, 660
 Fusco-Femiano, R., Dal Fiume, D., Feretti, L., Giovannini, G., Grandi, P., Matt, G., Molendi, S., & Santangelo, A. 1999, *ApJ*, 513, L21
 Fusco-Femiano, R., et al. 2000, *ApJ*, 534, L7
 Kang, H., Rachen, J. P., & Biermann, P. L. 1997, *MNRAS*, 286, 257
 Kayo, I., Taruya, A., & Suto, Y. 2001, *ApJ*, 561, 22
 Kitayama, T. 1997, Ph.D. thesis, Univ. Tokyo
 Lacey, C., & Cole, S. 1993, *MNRAS*, 262, 627 (LC)
 Lahav, O., Lilje, P. B., Primack, J. R., & Rees, M. J. 1991, *MNRAS*, 251, 128
 Levinson, A. 1994, *ApJ*, 426, 327
 Lieu, R., Mittaz, J. P. D., Bowyer, S., Breen, J. O., Lockman, F. J., Murphy, E. M., & Hwang, C.-Y. 1996, *Science*, 274, 1335
 Markevitch, M., Gonzales, A. H., David, L., Vikhlinin, A., Murray, S., Forman, W., Jones, C., & Tucker, W. 2002, *ApJ*, 567, L27
 Markevitch, M., Sarazin, C. L., & Vikhlinin, A. 1999, *ApJ*, 521, 526
 Markevitch, M., & Vikhlinin, A. 2001, *ApJ*, 563, 95
 McClements, K. G., Dendy, R. O., Bingham, R., Kirk, J. G., & Drury, L. O'C. 1997, *MNRAS*, 291, 241
 Miniati, F., Jones, T. W., Kang, H., & Ryu, D. 2001a, *ApJ*, 562, 233
 Miniati, F., Ryu, D., Kang, H., Jones, T. W. 2001b, *ApJ*, 559, 59
 Miniati, F., Ryu, D., Kang, H., Jones, T. W., Cen, R., & Ostriker, J. P. 2000, *ApJ*, 542, 608
 Nakamura, T. T., & Suto, Y. 1997, *Prog. Theor. Phys.*, 97, 49
 Ohno, H., Takizawa, M., & Shibata, S. 2002, *ApJ*, 577, 658
 Petrosian, V. 2001, *ApJ*, 557, 560
 Press, W. H., & Schechter, P. 1974, *ApJ*, 187, 425 (PS)
 Roettiger, K., Burns, J. O., & Stone, J. M. 1999, *ApJ*, 518, 603
 Salvador-Solé, E., Solanes, J. M., & Manrique, A. 1998, *ApJ*, 499, 542
 Sarazin, C. L. 1999, *ApJ*, 520, 529
 Sarazin, C. L., & Kempner, J. C. 2000, *ApJ*, 533, 73
 Schlickeiser, R., Sievers, A., & Thiemann, H. 1987, *A&A*, 182, 21
 Sheth, R. K., & Diaferio, A. 2001, *MNRAS*, 322, 901
 Sreekumar, P., et al. 1996, *ApJ*, 464, 628
 Takizawa, M. 1999, *ApJ*, 520, 514
 Takizawa, M., & Naito, T. 2000, *ApJ*, 535, 586
 Volk, H. J., Aharonian, F. A., & Breitschwerdt, D. 1996, *Space Sci. Rev.*, 75, 279